Applied Radiation and Isotopes 167 (2021) 109439

Contents lists available at ScienceDirect

Applied Radiation and Isotopes

journal homepage: http://www.elsevier.com/locate/apradiso

PSMA targeted conjugates based on dextran

Magdalena Janczewska [a,b,*], Michał Szkop [a], Grzegorz Pikus [a,c], Konstancja Kopyra [a], Anna Świątkowska [a], Kamil Brygoła [a], Urszula Karczmarczyk [d], Jarosław Walczak [a,f], Michał Tomasz Żuk [a,e], Jolanta Duszak [a,b], Tomasz Ciach [a,b]

[a] NanoThea Inc., Rakowiecka 36, 02-532 Warsaw, Poland
[b] Warsaw University of Technology, Faculty of Chemical and Process Engineering, Waryńskiego 1, 00-645 Warsaw, Poland
[c] Institute of Organic Chemistry, Polish Academy of Sciences, Kasprzaka 44/52, 01-224 Warsaw, Poland
[d] National Centre for Nuclear Research Radioisotope Centre POLATOM, Andrzeja Sołtana 7, 05-400 Otwock, Poland
[e] University of Warsaw, Faculty of Chemistry, Pasteura 1, 02-093 Warsaw, Poland
[f] Institute of Fundamental Technological Research, Polish Academy of Sciences, Pawińskiego 5b, 02-106 Warsaw, Poland

ARTICLE INFO

Keywords:
Dextran
Radioconjugates
Nanoparticles
Prostate cancer
DOTA-Conjugates

ABSTRACT

Background: Currently, radiotherapy is one of the most popular choices in clinical practice for the treatment of cancers. While it offers a fantastic means to selectively kill cancer cells, it can come with a host of side effects. To minimize such side effects, and maximize the therapeutic effect of the treatment, we propose the use of targeted radiopharmaceuticals. In the study presented herein, we investigate two synthetic pathways of dextran-based radiocarriers and provide their key chemical and physical properties: stability of the bonding of chelating agent and tertiary structure of obtained formulations and its influence on biological properties. Additionally, PSMA small molecule inhibitor was attached and quantified using DELFIA fluorescence assay. Finally, biological properties and radiolabeling yield were studied using confocal microscopy and ITLC-SG chromatography.

Results: Two types of Dex-conjugates – micelle-like nanoparticles (NPs) and non-folded conjugates – were successfully generated and shown to exhibit cellular effects. The tertiary structure of the conjugates was found to influence the selectivity of PSMA and mediate cell binding as well as cellular uptake mechanisms. NPs were shown to be internalized by other, non – PSMA mediated channels. Simultaneously, the uptake of non-folded conjugates required PSMA inhibitor to pass through cell membrane. The radiochemical yield of NHS coupled DOTA chelator was between 91.3 and 97.7% while the TCT-amine bonding showed higher stability and gave the yields of 99.8–100%.

Conclusions: We obtained novel, dextran-based radioconjugates, and presented a superior method of chelator binding, resulting in exquisite radiochemical properties as well as selective cross-membrane transport.

1. Authorship statement

MJ designed the study and was a major contributor in writing the manuscript. MS obtained conjugates and performed PSMA quantative analysis. GP performed GuL synthetic modification as well as synthesis of nanoparticles. KK and JD provided physico-chemical analysis, DOTA quantative measurements and purification of all formulations. AŚ and JW performed cytotoxicity analysis and binding visualization preceded by evaluation of PSMA expression in selected cell lines. KB obtained Cy5 stained conjugates and analysis of thereof. UK performed radiolabelling and radio stability experiments. MTŻ supported work of UK in establishing radiolabelling and radio stability protocols. TC provided critical review of the manuscript and results. All authors read and approved the final manuscript.

2. Background

Cancer is regarded as one of civilization's most common diseases and one of the leading causes of death worldwide. Its treatment remains extremely challenging due to the complex nature of the disease. Yearly, numerous drugs and combination therapies are investigated, alongside the development of powerful data analysis tools, to improve the way we handle cancer. Radionuclides have been a part of this therapeutic process for decades, and are now frequently used in diagnoses. However,

* Corresponding author. Jaszowiecka 6/28 02Warsaw, Poland.
E-mail address: m.m.janczewska@gmail.com (M. Janczewska).

https://doi.org/10.1016/j.apradiso.2020.109439
Received 1 April 2020; Received in revised form 6 August 2020; Accepted 22 September 2020
Available online 2 October 2020
0969-8043/

radioisotopes have recently gained special interest as a chemotherapeutic drug alternative, through encapsulation and precise transport to cancer tissues.

Different approaches towards brachytherapy – delivery of active radionuclide to an organ – have been reported in literature. Human and chimeric (humanized) antibodies with attached bifunctional chelators (e.g. DOTA) are currently being used to create highly specific conjugates. Multiple small molecules with receptor binding moieties have been developed to target different membrane receptors, such as Prostate Specific Membrane Antigen (PSMA) and Human Epidermal growth factor receptor 2 (HER2).

In this work we focus on polymeric, particularly dextran, conjugates as radionuclide carriers. Dextran, a polysaccharide composed of glucose monomers with side glucose chains, is already used clinically as blood expander and has been granted Food and Drug Administration (FDA) approval for intravenous administration. Dextran is commercially produced using bacteria, significantly lowering the cost of the polymer, and then further purified to a pharmacological grade. Following the [^{18}F] fluodeoxyglucose (FDG) strategy of exploiting glucose as a "targeting" molecule, we propose the use of dextran due to the presence of glucose at the end of every chain. In 1920, Otto Warburg and his colleagues observed that tumor cells consume vast amounts of glucose compared to the surrounding tissues. They also reported lactate production, despite the unlimited oxygen access to the of cells, concluding that cancer cells exhibited aerobic glycolysis due to the need of intensive proliferation. Further studies confirmed two metabolic pathways of cancer metabolism and showed that both mechanisms needed to be blocked to impair tumor growth (Liberti and Locasale, 2016).

Several research groups have also reported studies using dextran as a radionuclide carrier. Two radiolabeling approaches were introduced from these studies: those with bifunctional chelators and those without. Gholipour et al. proposed to oxidize the dextran, obtaining carboxylic groups, which in the next step bind a [^{68}Ga] radionuclide (Gholipour et al., 2019). A second radiolabeling strategy of ^{68}Ga was also proposed by the Almasi research group, where dextran chains were first oxidized to obtain aldehyde groups, followed by a Maillard reaction with thiosemicarbazone. These thiosemicarbazone groups were reported to create complexes with metals, such as Gallium (III), with authors evaluating the radiolabeling efficacy to be over 95% (Almasi et al., 2019). A different coordination strategy was introduced by Du et al. (2000) where, similar to Almasi et al.'s approach, dextran was oxidized to form aldehydes, followed by Schiff base creation with cysteine. Subsequently the imine bonds were reduced to create stable covalent bonds. Cysteine moieties were used as chelating compounds for ^{188}Re, at first giving a high radiolabeling purity (over 95%) but releasing the radionuclide in the presence of cysteine solution (Du et al., 2000). Several other research groups have investigated different methods of forming stable bonds to radionuclide is via bifunctional chelators. Two of these groups, used dextran as Magnetic Resonance Imaging (MRI) contrast agent with Gadolinium. Corot et al. (1997) functionalized carboxymethyldextran with a Gd-DOTA macrocyclic complex via the addition of an amino spacer. The Hals research group also used dextran with conjugated Gd-DTPA, but unlike Corot et al. directly bound the Gd-DTPA to hydroxyl groups or via a β-alanine linking group. Comparing the two conjugates in vivo, the conjugate with alanine spacer between dextran and chelator was observed to significantly prolong the conjugate half-life in the plasma (Petter et al., 2013). A similar approach was suggested by Holmberg et al. (2018), where dextran was conjugated with DOTA via a lysine as a spacer, however no data regarding the metal labelling (authors used Gd as a model isotope) or binding details were revealed. Finally, dextran chains were applied as a coating to or as a backbone of nanoparticles. The research group of Jarret used dextran sulfate to coat iron oxide nanoparticles dedicated to MRI and PET (Positron-Emission Tomography) scans. For PET, the DOTA chelator was coupled and radiolabeled with the ^{64}Cu isotope however, the yield of this labelling process was below 22% (Jarrett et al., 2008). Single chain dextran nanoparticles were prepared by Gracia et al. (2017), with the dextran chain modified to introduce methacrylate moieties with subsequent crosslinking using 3,6-dioxa-1,8-octane-dithiol. The obtained nanoparticles could be further modified with functional groups to control physical properties such as zeta potential. Authors used NODA (1,4,7-triazacyclononane-1,4-diacetic acid) as a chelator and radiolabeled nanoparticles with ^{67}Ga for SPECT (Single-Photon Emission Computerized Tomography), obtaining a yield of 51% and a high stability in buffer (over 95% at 48 h after labelling).

Table 1
Characteristics of obtained Dex-conjugates.

Formulation	Content of DOTA [nmol/mg]	Yield of DOTA conjugation [%]	Content of Cy5 [nmol/mg]	Size [nm]	Zeta potential [mV]
PAD 0%GuL	126.07	52	–	111.7 ± 31.4	−3.03 ± 1.75
PAD 5%GuL	70.96	29	–	147.2 ± 8.4	−2.04 ± 0.25
PAD 30% GuL	49.29	20	–	124.0 ± 10.4	−9.01 ± 0.22
PAD 50% GuL	32.63	13	–	80.0 ± 20.9	−10.00 ± 0.35
PAD 5%GuL Cy5	–	–	1.37	–	–
PAD 50% GuL Cy5	–	–	2.27	–	–
DX-TCT 0% GuL	216.7	80	–	–	–
DX-TCT 5% GuL	237.1	88	–	–	–
DX-TCT 30% GuL	205.9	76	–	–	–
DX-TCT 50% GuL	187.0	70	–	–	–
DX-TCT 5% GuL Cy5	–	–	7.31	–	–
DX-TCT 50% GuL Cy5	–	–	7.23	–	–

In the present work, we propose two methods of dextran modification for chemical binding of a chelator. In order to evaluate the chemical stability of the DOTA conjugation, radiolabeling and radio stability studies were performed with lutetium-177. The conjugates generated were also labelled with a Cy5 (Cyanine 5) fluorescent probe and a PSMA specific inhibitor (GuL) to investigate the receptor-specific uptake of conjugates by prostate cancer cells. Experiments were performed on PSMA+ and PSMA-cell lines as well as with 2-PMPA (2-Phosphonomethyl pentanedioic acid), a competitive inhibitor for the PSMA membrane protein.

3. Methods

3.1. Dextran oxidation to polyaldehydedextran (PAD) (5)

Dextran (10.00 g, 70 kDa, Pharmacosmos) was dissolved in 200 mL of ultra-pure water to which sodium metaperiodate (1.32 g, 6.17 mmol, Sigma Aldrich) was added. The reaction mixture was stirred in the dark at room temperature for 1 h, and the reaction product was subsequently dialyzed (MWCO 12–14 kDa, Carl Roth) against 100-fold excess of ultra-pure water for 72 h (until the complete purification of periodate ions) and dried in the oven at 40 °C.

3.2. Synthesis of tri(tert-butyl) ester of GuL-PEG5-NHBoc (3)

In a round-bottom flask (25 mL) BocNH-PEG5-NHS (104 mg, 0.205 mmol, BroadPharm) and tri (*tert*-butyl) ester of Glu-urea-Lys (100 mg, 0.205 mmol, ABX) were dissolved in 5 mL of dry DCM. DIPEA (26.5 mg, 36 μL, 0.205 mmol, Sigma Aldrich) was then added to the solution. The

Table 2
Radiochemical stability of ^{177}Lu-labelled **Dex-conjugates** stored at room temperature (22 ± 2 °C) and human serum at 37 ± 1 °C.

Formulation	Radiochemical stability of radiolabeled Dex-conjugates stored in RT (free lutetium-177 [%])					Radiochemical stability of radiolabeled Dex-conjugates stored in human serum at 37 °C (free lutetium-177 [%])				
	1 h	24 h	48 h	72 h	144 h	1 h	24 h	48 h	72 h	144 h
PAD 0%GuL	97.7 ± 0.5 (0.0 ± 0.0)	98.5 ± 0.8 (0.0 ± 0.0)	96.4 ± 2.5 (0.1 ± 0.1)	94.2 ± 1.3 (0.3 ± 0.1)	n.d.	96.2 ± 0.8 (0.0 ± 0.0)	97.3 ± 0.9 (0.0 ± 0.0)	97.2 ± 0.2 (0.4 ± 0.1)	94.5 ± 2.3 (0.7 ± 0.1)	n.d.
PAD 5%GuL	93.4 ± 0.8 (0.4 ± 0.1)	96.2 ± 0.9 (0.9 ± 0.5)	95.5 ± 0.9 (0.4 ± 0.2)	91.1 ± 2.8 (0.7 ± 0.2)	n.d.	91.8 ± 0.9 (0.0 ± 0.0)	95.8 ± 0.1 (0.0 ± 0.0)	92.1 ± 0.3 (2.2 ± 0.2)	n.d.	n.d.
PAD 30%GuL	91.3 ± 1.1 (0.5 ± 0.2)	90.9 ± 1.0 (0.9 ± 0.2)	89.2 ± 0.5 (0.6 ± 0.1)	n.d.	n.d.	92.3 ± 3.6 (0.0 ± 0.0)	86.7 ± 2.4 (3.2 ± 2.5)	83.0 ± 1.3 (3.9 ± 0.3)	n.d.	n.d.
PAD 50%GuL	n.d.	n.d.	n.d.	n.d.	n.d.	n.d.	n.d.	n.d.	n.d.	n.d.
DX-TCT 0% GuL	99.9 ± 0.1 (0.1 ± 0.0)	100.0 ± 0.0 (0.0 ± 0.0)	99.4 ± 0.6 (0.6 ± 0.1)	98.1 ± 1.6 (0.8 ± 0.3)	93.7 ± 1.3 (0.7 ± 0.2)	100.0 ± 0.0 (0.0 ± 0.0)	100.0 ± 0.0 (0.0 ± 0.0)	100.0 ± 0.0 (0.0 ± 0.0)	100.0 ± 0.0 (0.0 ± 0.0)	98.3 ± 0.2 (0.6 ± 0.2)
DX-TCT 5% GuL	99.8 ± 0.1 (0.2 ± 0.2)	99.1 ± 0.6 (0.4 ± 0.4)	100.0 ± 0.0 (0.0 ± 0.0)	99.2 ± 0.5 (0.3 ± 0.2)	98.7 ± 0.4 (0.4 ± 0.2)	100.0 ± 0.0 (0.0 ± 0.0)	99.7 ± 0.1 (0.3 ± 0.1)	100.0 ± 0.0 (0.0 ± 0.0)	100.0 ± 0.0 (0.0 ± 0.0)	98.9 ± 0.4 (0.4 ± 0.2)
DX-TCT 30% GuL	100.0 ± 0.0 (0.0 ± 0.0)	99.9 ± 0.1 (0.1 ± 0.0)	99.8 ± 0.3 (0.2 ± 0.1)	99.2 ± 0.4 (0.3 ± 0.1)	98.6 ± 0.3 (0.4 ± 0.3)	100.0 ± 0.0 (0.0 ± 0.0)	99.4 ± 0.2 (0.6 ± 0.2)	100.0 ± 0.0 (0.0 ± 0.0)	100.0 ± 0.0 (0.0 ± 0.0)	99.1 ± 0.3 (0.4 ± 0.2)
DX-TCT 50% GuL	100.0 ± 0.0 (0.0 ± 0.0)	99.9 ± 0.1 (0.1 ± 0.0)	99.9 ± 0.1 (0.1 ± 0.0)	99.4 ± 0.2 (0.1 ± 0.0)	99.0 ± 0.4 (0.3 ± 0.1)	100.0 ± 0.0 (0.0 ± 0.0)	100.0 ± 0.0 (0.0 ± 0.0)	100.0 ± 0.0 (0.0 ± 0.0)	100.0 ± 0.0 (0.0 ± 0.0)	100.0 ± 0.0 (0.0 ± 0.0)

n.d. – no data.

Table 3
Amounts of reagents used for synthesis of **PAD-GuL-DOTA** and **PAD-GuL-Cy5** nanoparticles.

Formulation	Reagents [mg]							
	1	2	DIPEA	PAD (5)[a]	DAD·2HCl	$NaBH_4$	DOTA[b, c]	$Cy5NH_2$
PAD 0%GuL	-	-	-	338.0	44.2	12.2	24.3	-
PAD 5%GuL	10.0	10.4	2.7	857.0	106.4	31.0	24.3	-
PAD 30%GuL	10.0	10.4	2.7	142.9	13.1	5.2	24.3	-
PAD 50%GuL	20.0	20.8	5.4	171.4	11.2	6.2	24.3	–
PAD 5%GuL Cy5	10.0	10.4	2.7	857.0	103.1	–	–	8.0
PAD 50%GuL Cy5	10.0	10.4	2.7	85.7	5.3	–	–	0.8

[a] 478.3 nmol of CHO/mg
[b] Used as **DOTA-NHS**
[c] Used for 100 mg of obtained **PAD-GuL**.

reaction mixture was stirred at RT for 24 h. The solvent was evaporated, and the oily residue chromatographed on a silica gel column.

3.3. Synthesis of *PAD-GuL* nanoparticles (6)

Four different formulations of PAD-GuL nanoparticles with various content of the GuL-PEG5-NH_2 targeting agent (deprotected **3**) attached to PAD were prepared, i.e. formulations with a GuL-PEG5-NH_2 substitution of 0,5%, 30% and 50% (Table 3). Appropriate amounts of GuL-PEG5-NH_2 substrate, required to obtain nanoparticles with a specific substitution degree, were calculated based on the content of aldehyde groups in the PAD (478.3 nmol/mg). The remaining aldehyde groups in the PAD were substituted with a 1,10-diaminodecane (DAD) serving as a coiling agent – due to long carbon chain promotes folding of PAD chain into trietary form of nanoparticles. As an exemple of the PAD-5%GuL synthesis: in a round-bottom flask (5 mL) BocNH-PEG5-NHS (10,4 mg, 0.0205 mmol) and tri (*tert*-butyl) ester of Glu-urea-Lys (10,0 mg, 0.0205 mmol) were dissolved in 0.5 mL of dry DCM. Then DIPEA (2.65 mg, 4 mL, 0.0205 mmol) was added. The reaction mixture was stirred at RT for 24 h. Next, TFA (187.0 mg, 125 mL, 1.64 mmol, Sigma Aldrich) was added and the reaction mixture was stirred for another 24 h. Subsequently, the solvent was evaporated, the oily residue dissolved in 0.5 mL of ultra-pure water, and the pH adjusted to ~11.0. The aqueous solution of GuL-PEG5-NH2 was immediately added to the solution of PAD (854 mg, 0.410 mmol of CHO groups) in 8.5 mL of ultra-pure water. The pH of the reaction mixture was adjusted to ~11.0, using 0.5 M NaOH solution, and stirred at 30 °C for 1 h. Next, 1,10-diaminodecane dihydrochloride (106.44 mg, 0.385 mmol, Sigma Aldrich) was added as a solution in 2.27 mL of ultra-pure water. The pH was adjusted to ~11.0 and the reaction mixture was stirred at 30 °C for 100 min (pH was monitored and adjusted to ~11.0, every 20 min). The reaction was stopped by adjusting pH to ~7.4 using 0.5 M HCl solution. Next, the solution of sodium borohydride (31.0 mg, 0.820 mmol) in 3.2 mL of ethanol was added and the reaction mixture was stirred at 37 °C for 1 h. Finally, the pH of the reaction mixture was again adjusted to 7.4, the reaction product (PAD-GuL) dialyzed against acetate buffer (10 mM, pH 5.0) for 24 h and subsequently against ultra-pure water for another 24 h, and freeze-dried. Water or buffer was changed 3 times during each 24 h of dialysis. The volume of dialysate was used in at least a 100-fold excess of the volume of the reaction mixture.

3.4. DOTA conjugation to *PAD-GuL* nanoparticles (7)

Lyophilized nanoparticles (100 mg) were dissolved in 2.0 mL of 0.1 M phosphate buffer pH 8.0. Next, DOTA-NHS (18.5 mg, 24.3 mmol), dissolved in 0.5 mL of ultra-pure water, was added. The reaction mixture was stirred at RT for 1.5 h. The reaction product (PAD-GuL-DOTA) was subsequently dialyzed against acetate buffer (10 mM, pH 5.0) for 24 h and then against ultra-pure water for another 24 h and finally freeze-dried. Water or buffer was changed 3 times during each 24 h of dialysis. The volume of dialysate was used in at least a 100-fold excess of the volume of the reaction mixture.

3.5. Dextran activation with trichlorotriazine (8)

Dextran (2.5 g, 70 kDa) was dissolved in 150 mL of ultra-pure water and 625 mg of trichlorotriazine (TCT, Sigma Aldrich) in 3.75 mL of acetone (16.7% w/v solution) was added to this solution. The reaction was carried out at 4 °C with stirring and the pH of the reaction mixture was maintained above 7.5 by addition of 1 mL portions of 0.5 M NaOH

Table 4
Amounts of reagents used for synthesis of **Dex-TCT-GuL-DOTA** and **Dex-TCT-GuL-Cy5** conjugates.

Formulation	Reagents [mg]						
	1	2	DIPEA	DEX-TCT (8)[a]	DOTA[b]	Gly	Cy5NH$_2$
DX-TCT 0% GuL	-	-	-	254.0	43.1	5.1	-
DX-TCT 5% GuL	10.0	10.4	2.7	762.1	127.7	13.9	–
DX-TCT 30% GuL	10.0	10.4	2.7	127.0	21.3	1.0	–
DX-TCT 50% GuL	20.0	20.8	5.4	152.4	25.5	–	–
DX-TCT 5% GuL Cy5	10.0	10.4	2.7	762.1	–	28.3	8.0
DX-TCT 50% GuL Cy5	10.0	10.4	2.7	76.2	–	1.5	0.8

[a]) 538.0 nmol of active chloride atoms/mg; [b]) used as DOTA-PEG$_4$-NH$_2$.

solution. The reaction was regarded as complete when no further changes in pH were observed. Obtained product (**Dex-TCT**) was subsequently dialyzed against ultrapure water for 24 h (water was changed 3 times, 100-fold excess of dialysate) and freeze-dried.

3.6. Synthesis of *Dex-TCT-GuL-DOTA* conjugates (*9*)

Similarly, to **PAD-GuL-DOTA** nanoparticles, four different formulations of **Dex-TCT-GuL-DOTA** were prepared, differing in the content of the GuL-PEG5-NH$_2$ targeting agent (deprotected **3**) attached to **Dex-TCT**, namely the formulations with a GuL-PEG5-NH$_2$ substitution of 0,5%, 30% and 50%. Appropriate amounts (Table 4) of GuL-PEG5-NH$_2$ substrate, required to obtain conjugates with a specific substitution degree, were calculated based on the content of the active chloride atoms in **Dex-TCT** (538.0 nmol/mg). The remaining active chloride atoms were substituted with a DOTA-PEG4-NH2 chelator (CheMatec) (50% of the substitution degree in each formulation) and glycine (50%, 45%, 20% and 0%). The latter was used to saturate the remaining active chloride atoms. The reactions were carried out at 60 °C for 3 h in 0.44 M carbonate buffer pH 8.4.125 mg of **Dex-TCT** in the total volume of 3.3 mL was used in each reaction. The obtained product (**Dex-TCT-GuL-DOTA**) was subsequently dialyzed against acetate buffer (10 mM, pH 5.0) for 24 h, then against ultra-pure water for another 24 h and finally, freeze-dried. Water or buffer was changed 3 times during each 24 h of dialysis. The volume of dialysate was used in at least a 100-fold excess of the volume of the reaction mixture.

3.7. Synthesis of *PAD-GuL Cy5* nanoparticles and *Dex-TCT-GuL Cy5* conjugates (*10, 11*)

For cellular uptake analyses, two formulations of **PAD-GuL-Cy5** and two formulations of **Dex-TCT-GuL-Cy5** were prepared. The synthesis procedures were as described above for **PAD-GuL** and **Dex-TCT-GuL** with DOTA chelator replacement with fluorescent dye Cy5 (Lumiprobe) and the substitution degrees were: GuL-PEG5-NH$_2$ 50%; Cy5 3%; DAD 47% or GuL-PEG5-NH$_2$ 5%; Cy5 3%; DAD 92% for **PAD-GuL-Cy5**, and GuL-PEG5-NH$_2$ 50%; Cy5 3%; glycine 47% or GuL-PEG5-NH$_2$ 5%; Cy5 3%; glycine 92% for **Dex-TCT-GuL-Cy5**. The obtained products (PAD-GuL-Cy5 and Dex-TCT-GuL-Cy5) were purified by dialysis against acetate buffer (10 mM, pH 5.0) supplemented with 50 mM NaCl for 24 h and subsequently against ultra-pure water for another 24 h, and freeze-dried. Water or buffer was changed 3 times during each 24 h of dialysis. The volume of dialysate was used in at least a 100-fold excess of the volume of the reaction mixture.

3.8. Quantification of aldehyde groups in *PAD* and active chloride atoms in *Dex-TCT*

The methods were based on the quantitative colorimetric determination of chromogenic derivatives, resulting from the reaction of hydroxylamine with 2,4,6-Trinitrobenzenesulfonic acid (TNBS). In order to quantify the aldehyde group content in **PAD** and the active chlorine atoms in **Dex-TCT**, both substances were incubated with hydroxylamine to react with mentioned groups. The remaining hydroxylamine was then quantified using TNBS.

3.9. Acquisition of the inhibition curves for *PAD-GuL-DOTA* and *Dex-TCT-GuL-DOTA* against PSMA

Inhibition curves against PSMA were obtained using a fluorimetric quantitative measurement of L-glutamate, which is released from *N*-acetyl-aspartyl-glutamate (NAAG, Sigma-Aldrich) in a PSMA catalyzed reaction (Zhang et al., 2006). The recombinant PSMA protein (Sino-Biological) was briefly incubated in the total solution volume of 50 μL with various amounts of **PAD-GuL-DOTA** or **Dex-TCT-GuL-DOTA** (i.e. 0; 0.05; 0.5; 5; 10; 25; 50; 500 and 5000 ng), in the presence of 10 μM NAAG for 150 min at 37 °C. Subsequently, 50 μL of Amplex™ Red Glutamic Acid/Glutamate Oxidase Assay Kit (ThermoFisher) solution containing 26 μg/mL of Amplex red (10-Acetyl-3,7-dihydroxyphenoxazine), 0.16 U/mL of L-glutamate oxidase, 0.5 U/mL of L-glutamate-pyruvate transaminase, 0.25 U/mL of horseradish peroxidase and 200 μM alanine were added. The samples were then incubated for 30 min in the dark at 37 °C, and the fluorescence was measured using Tecan Spark microplate reader with excitation and emission wavelengths at 530 and 590 nm, respectively.

3.10. Determination of DOTA chelator content in *PAD-GuL-DOTA* and *Dex-TCT-GuL-DOTA*

The DOTA chelator content was measured with an assay developed in our laboratory, relying on the quantitative determination of europium (Eu^{3+}) ions using DELFIA Enhancement Solution (PerkinElmer). The detailed assay procedure was reported in Szkop et al. (2019).

3.11. Cell culture model

The LNCaP, PC3 prostate cancer cells and human fibroblasts (all ATCC) were cultured in a controlled environment (5% CO_2 at 37 °C) and in specific media supplemented with 10% FBS and antibiotics (1% penicillin-streptomicin). LNCaP cells were maintained in RPMI (ATCC modification), PC3 cells in F12K, and fibroblasts in DMEM High glucose.

3.12. Cellular uptake

Cellular uptake of the synthetized PSMA targeted Dex-conjugates was visualized by confocal laser scanning microscopy. For these observations, LNCaP and PC3 cells were seeded on poly-L-lysine coated coverslips and left to attach and grow for 72 h in standard cell culture conditions. Then cells were treated with **PAD-GuL-Cy5** or **Dex-TCT-GuL-Cy5** at the concentration of 100 μg/mL for 30 or 60 min at 37 °C, fixed in 4% paraformaldehyde solution in PBS and mounted with ProLong Diamond Antifade Mountant with DAPI (Molecular Probes). Microscope slides were examined using a ZEISS LSM 880 Confocal Laser Scanning Microscope. The specificity of uptake was further verified by performing cell treatments with formulations at 4 °C, or after pre-incubation (30 min) in the presence of the PSMA inhibitor 2-PMPA (Cayman Chemical Company) (1 mM).

3.13. Cytotoxicity studies

XTT reagent (Thermo Fisher Scientific) was used to evaluate cell

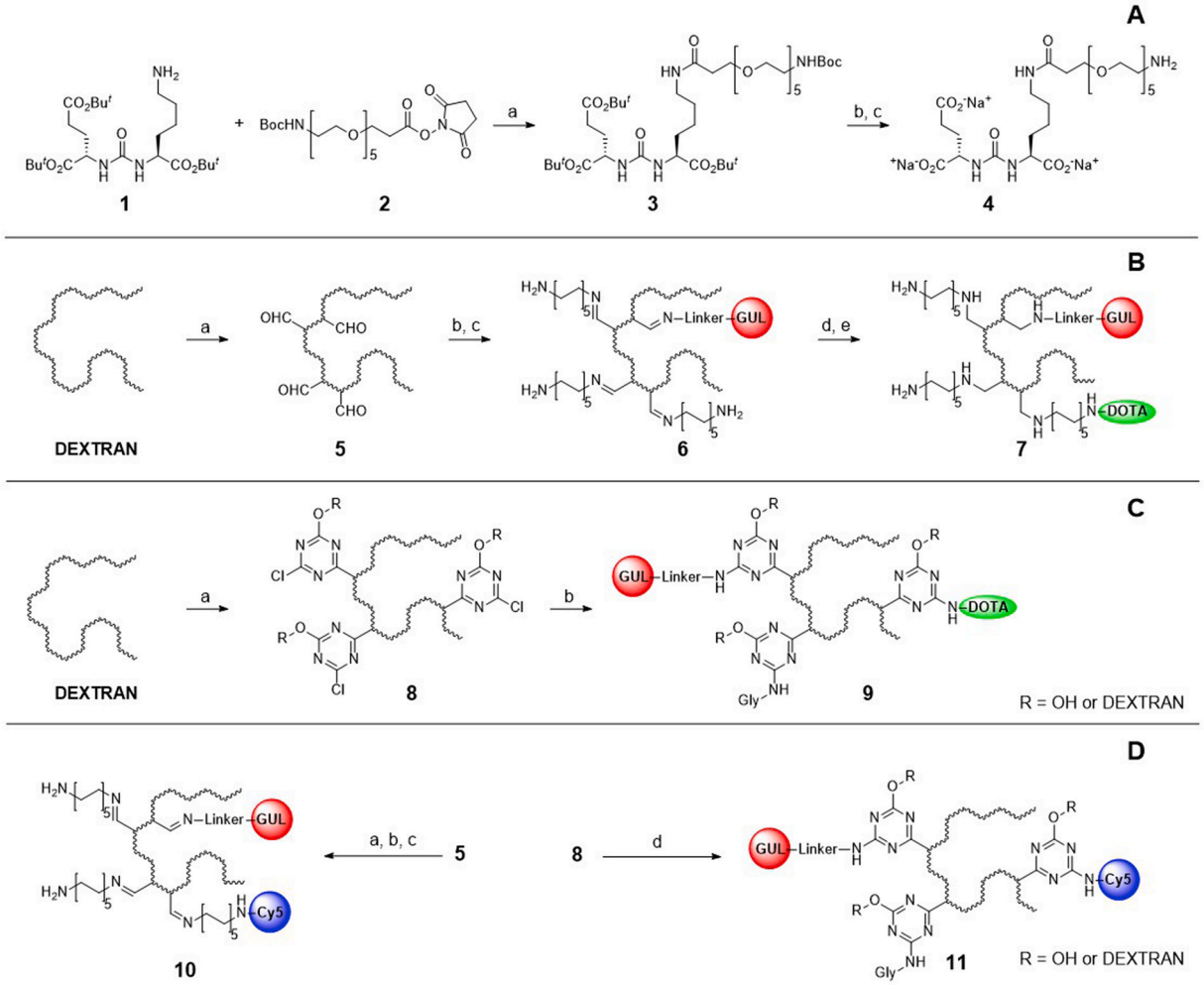

Scheme 1. **A** Modification of Glu-urea-Lys: a) DIPEA, DCM, RT, 24 h; b) TFA, DCM, RT, 24 h; c) $NaOH_{aq}$, pH~11; **B** Synthesis of **PAD GuL** NPs; a) $NaIO_4$, H_2O, RT, 60 min; b) GuL-PEG5-NH_2, pH~11, 35 °C, 60 min; c) DAD·2HCl, pH~11, 35 °C, 100 min; d) $NaBH_4$, EtOH, H_2O, pH~11, 35 °C, 60 min; e) DOTA-NHS, 0.1 M phosphate buffer, pH~11, RT, 90 min; **C** Synthesis of **Dex-TCT-GuL** conjugates: a) TCT, NaOH, H_2O 4–8 °C b) GuL-PEG5-NH_2, DOTA-PEG4-NH_2, Glycine, NaOH, 60 °C; **D** Synthesis of **PAD-GuL-Cy5** nanoparticles and **Dex-TCT-GuL-Cy5** conjugates: a) GuL-PEG5-NH_2, pH~11, 35 °C, 60 min; b) Cy5NH_2, pH~11, 35 °C, 60 min; c) DAD·2HCl, pH~11, 35 °C, 100 min; d) GuL-PEG5-NH_2, Cy5NH_2, Glycine, NaOH, 60 °C.

viability. To perform this analysis the LNCaP, PC3 cells and fibroblasts were seeded on 96 well plate in an appropriate culture medium and allowed to grow for 48 h. Subsequently, the culture medium was removed and replaced with fresh RPMI medium without FBS, supplemented with **PAD-GuL-DOTA** or **Dex-TCT-GuL-DOTA** in different concentrations (10, 50, 100, 250, 500 and 1000 μg/mL) or without supplementation (untreated control). Simultaneously, the XTT solution with PMS (Sigma Aldrich) was added to give a final concentration of 0.2 mg/mL. Absorbance measurements (λ = 450), using microplate spectrophotometer, took place after 4 h of incubation at 37 °C, 5% CO_2 in a humidified atmosphere. Possible interference was probed at each concentration of the Dex-conjugates by incubation with XTT in the RPMI medium without cells. For the 24 h incubation time points, samples were dissolved in a culture medium appropriate for each cell line but without serum supplementation. After the indicated time, the medium was replaced with XTT solution (0.2 mg/mL) in RPMI without FBS. Absorbance was measured after 2 h of incubation as specified earlier.

3.14. Radiochemistry

Dex-conjugates containing targeting agent and chelator (**PAD-GuL-DOTA** and **Dex-TCT-GuL-DOTA**) were radiolabeled with [^{177}Lu]$LuCl_3$ in 0.04 M HCl (LutaPol, POLATOM) of SA higher than 555 MBq/mg Lu. Radiolabeling was carried out in ascorbic acid sodium salt buffer (AAB; pH = 4.5–5) containing 2 mg of Dex-conjugates and 5–20 μL of [^{177}Lu]$LuCl_3$ (100–700 MBq), up to 1 mL. Reaction mixtures were incubated at 95 ± 5 °C for 15 min. The radiolabeling yield (RCY) of the final formulation was determined by thin layer chromatography. The thin-layer chromatography was performed on silica-gel plates (ITLC SG) with 0.1 M citric buffer (pH = 5) as a mobile phase to differentiate between the free ^{177}Lu (mobile phase) and Dex-conjugate bond ^{177}Lu (stationary phase). The radiolabeling yield was evaluated in the presence of a competitor (10 mM DTPA) in excess, which reacts with non-incorporated radionuclides. Due to a high RCY of radio conjugates, further purification was not necessary.

3.15. Serum stability assay

The in vitro stability of ^{177}Lu-Dex-conjugates was studied in human serum to assess the suitability of the formulation for pre-clinical use. For this, 200 μL portions of the radiolabelled Dex-conjugates were mixed with 1 mL of fresh human serum and incubated at 37 °C. The samples were analyzed by ITLC-SG after 1, 24 and 48 h of incubation using the method described above.

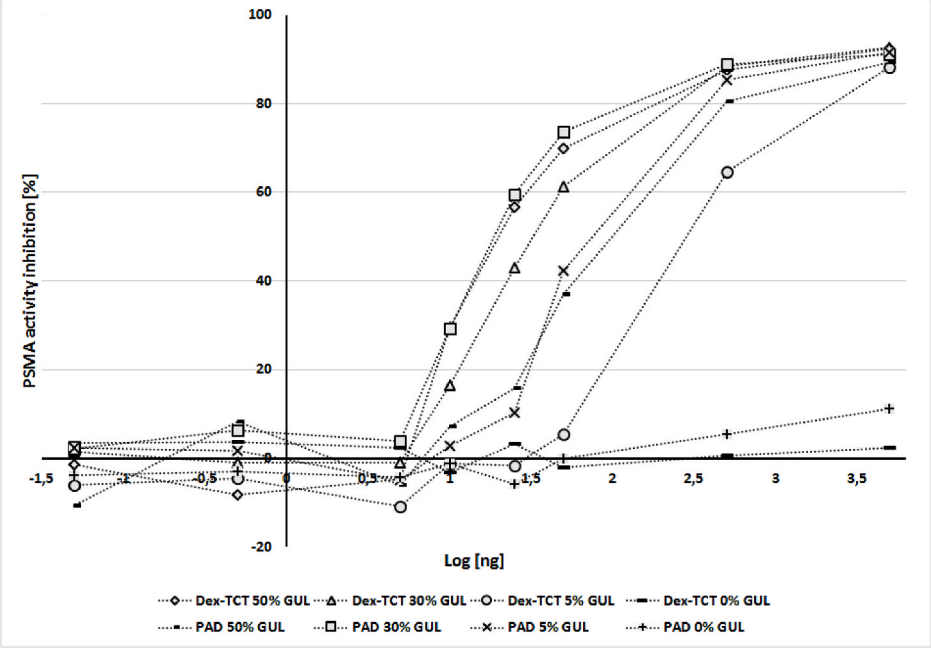

Fig. 1. Inhibition curves of **PAD-GuL-DOTA** and **Dex-TCT-GuL-DOTA** with various theoretical GUL substitutions.

4. Results

4.1. Synthesis

We present two pathways for the synthesis of dextran-based conjugates containing low-molecular weight PSMA inhibitor (GuL) and two types of indicators (DOTA chelator for radiolabeling studies and Cy5 dye for cell binding visualization). These two synthetic methods differ by way of molecular bonding, i.e. a classic procedure of reductive amination reactions vs. the nucleophilic aromatic substitution in trichlorotriazine. These two approaches resulted in two physical forms of products: **PAD-GuL-DOTA** nanoparticles and **Dex-TCT-GuL-DOTA** conjugates. Thus, we obtained two types of product for the targeted therapy of PC, containing varying amounts of Glu-urea-Lys (GuL) as a targeting agent for PSMA.

During the synthesis, we used an inactivated form of GuL—tri (*tert*-butyl) ester (**1**)—to modify its structure, by crosslinking with PEG linker (**2**) to lengthen amine arm (**3**). The next step was deprotection of *tert*-butyl ester groups by acid hydrolysis (**4**), followed by alkalization, to obtain the active form of modified inhibitor GuL-PEG5-NH_2 (**5**), ready for conjugation (Scheme 1A). Lengthening of the amine arm is required for the inhibitor to access the pocket of the PSMA active site. This is particularly crucial for nanoparticles as there is a need to expose the conjugated inhibiting agent on the surface of NPs.

By means of each synthetic route (i.e. with **PAD** and **Dex-TCT**) we have prepared four variants of DOTA-containing products with different amounts of GuL and two variants of Cy5 containing products with different amounts of GuL.

The initial step of nanoparticle synthesis was the partial oxidation of dextran, using sodium metaperiodate, to obtain polyaldehydedextran (**PAD**, **5**). This modification resulted in the presence of aldehyde groups in the polysaccharide chain that were further functionalized (Scheme 1B). GuL-derivative (**4**) and coiling agent DAD·2HCl were coupled to **PAD** by imine formation under basic conditions in water (**6**). The resulting micelle-type nanoparticles containing imine bonds were reduced using sodium borohydride. The primary amine groups were further functionalized with DOTA-NHS chelator (Scheme 1B) to give the target product (**7**). In order to obtain Cy5 labelled NPs, **PAD** was reacted with GuL-PEG5-NH_2 (**4**) under basic conditions, before an aqueous solution of Cy5NH_2 was added. The final step was the addition of DAD·2HCl to obtain imine-form of nanoparticles without reduction (**10**) (Scheme 1D).

The synthesis of the conjugates began with a reaction of Dex and TCT to give an activated form of dextran (**Dex-TCT**, **8**). Cyanuric chloride modified the structure of the polysaccharide via nucleophilic aromatic substitution of chlorine atoms in TCT under basic conditions at 4–8 °C. During this modification, 2 M equivalents of sodium hydroxide (in relation to TCT) were used, affording (**8**) upon completion. The amount of base corresponded to the two chlorine atoms which were substituted under described conditions. Consequently, we assumed that crosslinking or hydrolysis may occur. Because of this, one chlorine atom remained, in the triazine ring and was available for further modification by (**4**) and other components. GuL-PEG5-NH_2 and DOTA chelator (in this case an amine derivative) were combined with glycine, making a three-component mixture which reacted with **Dex-TCT** in alkaline conditions at 60 °C, affording the final product (**9**) (Scheme 1C). The procedure for the synthesis Dex-TCT-GuL-Cy5 (**11**) was similar and is presented in Scheme 1D.

The DOTA chelator content was quantified with a DELFIA assay. [11] It was observed that the levels of DOTA attachment to **PAD-GuL** NPs varied with the amount of added GuL and the yield decreased (from 52% to 13%) with greater substitution of GuL. The content of DOTA ranged from 126 to 33 nmol/mg of **PAD-GuL-DOTA**. The efficacy of DOTA bonding to **Dex-TCT** was not related to GuL content in the conjugate and proceeded in the yields of 70–88%. The content of DOTA ranged from 217 to 187 nmol/mg of **Dex-TCT-GuL-DOTA**. The **PAD-GuL NPs** and **Dex-TCT-GuL** conjugates labelled with Cy5 (i.e. **PAD-Gul-Cy5** and **c**) were obtained with variable amounts of (**5**) added to the reaction (5 and 50%) and a constant amount of Cy5. The determined amounts of Cy5 were 1.37 and 2.27 nmol/mg for **PAD-GuL-Cy5** and 7.31 and 7.23 nmol/mg for **Dex-TCT-GuL-Cy5**. The characteristics of these products is described in Table 1. Due to the fact that **Dex-TCT-GuL** conjugates do not form micelle-like structures, the measurements of size and zeta potential were not required.

4.2. PSMA inhibiting properties of nanoparticles and conjugates

In order to determine the inhibitory properties of **PAD-GuL-DOTA**

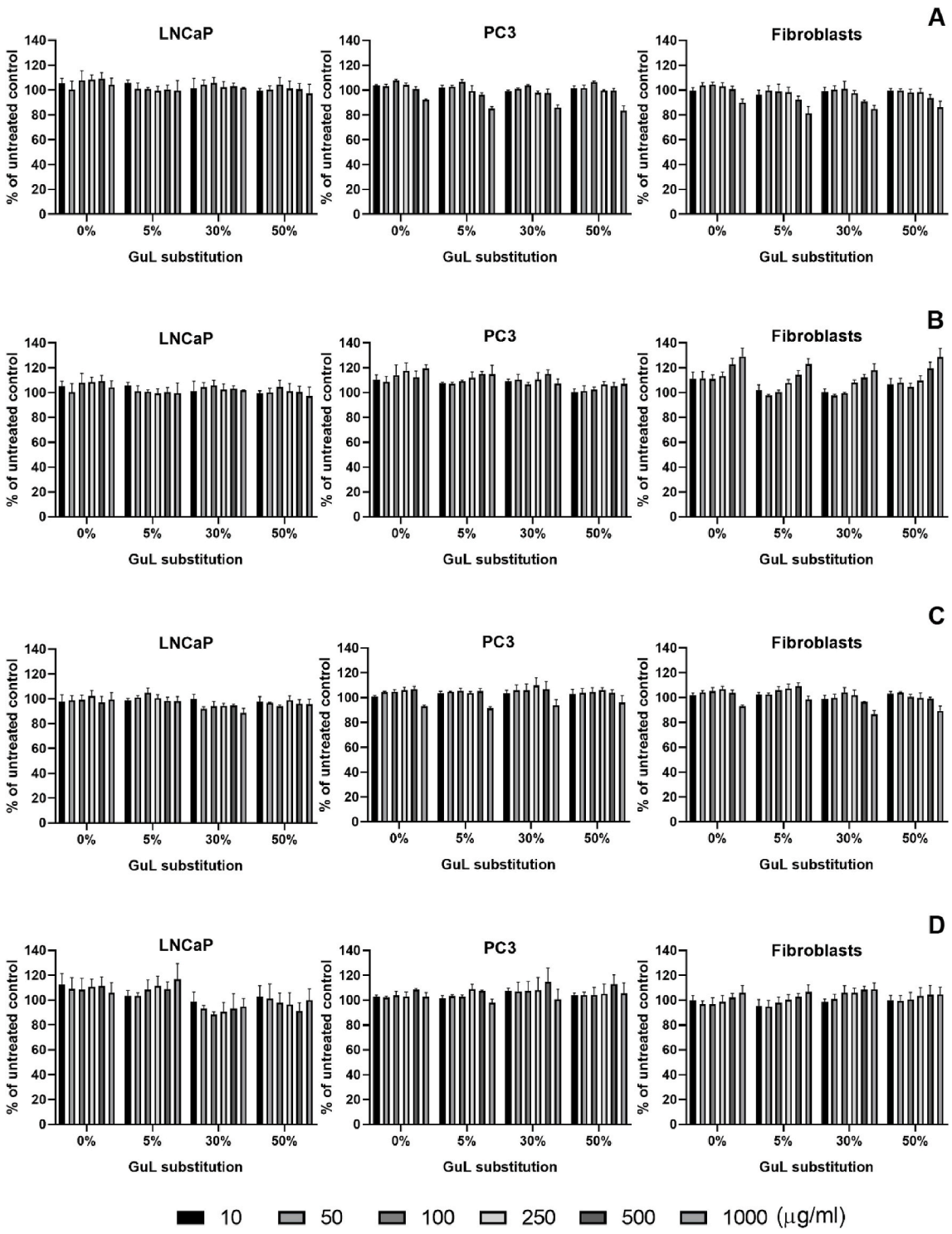

Fig. 2. Cell toxicity of synthesized formulations tested with XTT assay. LNCaP, PC3 and Fibroblasts treated with **PAD-GuL-DOTA** for 4 h (**A**), PAD-GuL-DOTA for 24 h (**B**), **Dex-TCT-GuL-DOTA** for 4 h (**C**), **Dex-TCT-GuL-DOTA** for 24 h (**D**). Results are expressed as a percentage of untreated control (mean ± SEM, n ≥ 3).

and **Dex-TCT-GuL-DOTA,** which corresponds to the content of GuL in the prepared formulations, we used the fluorimetric assay described above. As shown in Fig. 1, no substantial inhibition was observed for formulations where the theoretical substitution with GuL was 0%. For **Dex-TCT-GuL-DOTA** conjugates, the degree of inhibition increased gradually with a corresponding rise in theoretical substitution of GuL. For **PAD-GuL-DOTA**, the highest inhibitory properties were observed for formulation containing the theoretical substitution with GuL of 30%.

4.3. In vitro cell assays/cell viability

The potential toxicity of prepared formulations was verified on two prostate cancer cell lines, LNCaP and PC3, as well as on human dermal fibroblasts, which represent non-malignant cells. Results shown in Fig. 2 indicate that none of analyzed formulations are toxic for the investigated cell lines as neither Dex-conjugate caused a decrease in cell viability below the critical level of 80% of control. The strongest negative impact was observed after treatment of PC3 cells and Fibroblasts with **PAD-**

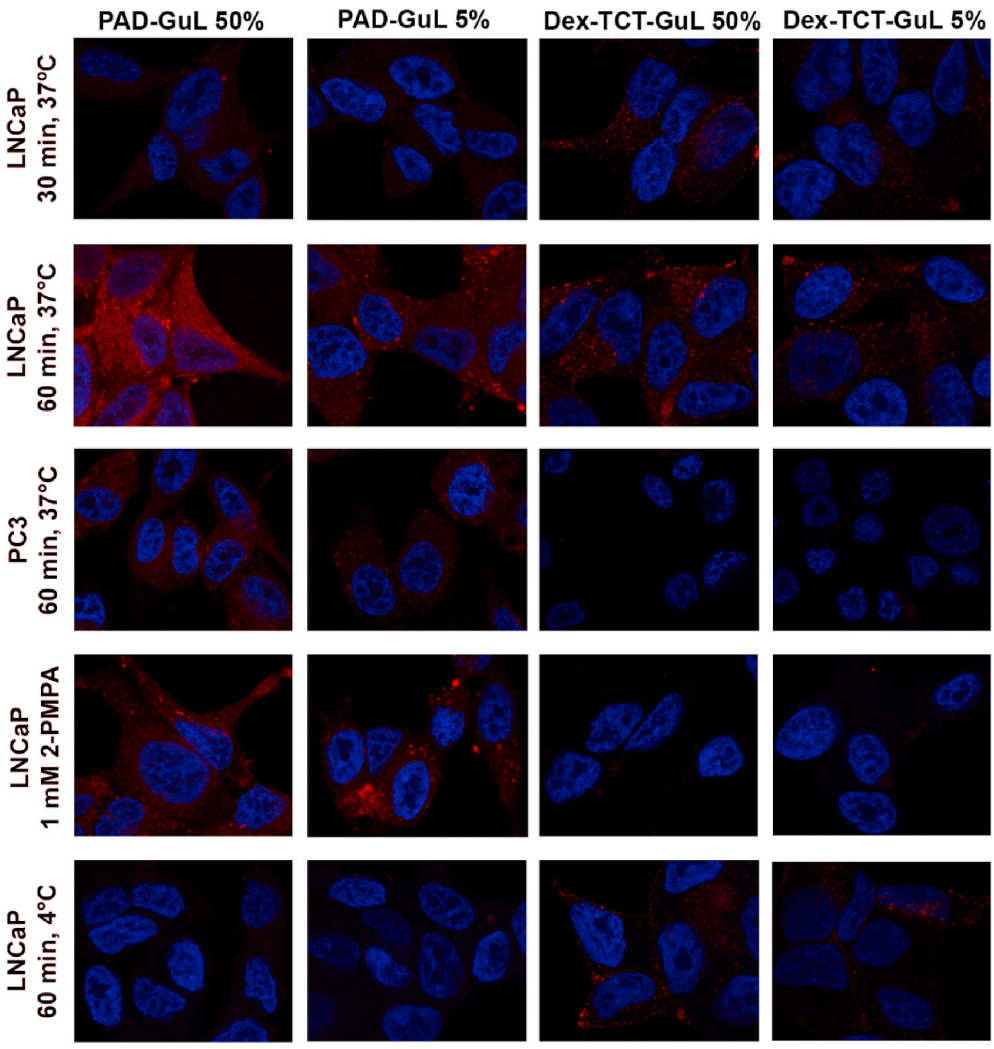

Fig. 3. Cell binding ability of prepared formulations. The formulations labelled with Cy5 – red, DAPI labelled nuclei – blue. (For interpretation of the references to colour in this figure legend, the reader is referred to the web version of this article.)

GuL-DOTA in the highest concentration (1000 μg/mL) for 4 h (Fig. 2A), when cells viability dropped below 85% of control. After 24 h of incubation, we did not observe a decline in PC3 cells viability (Fig. 2B) and, surprisingly, we even noticed the increase in case of fibroblasts. For LNCaP cells, treatment with **PAD-GuL-DOTA** for 4 or 24 h caused no significant changes in viability. Similarly, all **Dex-TCT** based formulations showed no obvious cytotoxicity to analyzed cell lines in the tested range of concentrations and time points.

4.4. Cellular uptake of Dex-conjugates

We used confocal microscopy and formulations labelled with Cy5 to visualize their binding ability to the cells (Fig. 3). The 50% and 5% GuL substituted formulations were chosen for studies and were incubated with LNCaP cells (PSMA+) for 30 or 60 min at 37 °C. Under these conditions, signals of **PAD-GuL-Cy5** and **Dex-TCT-GuL-Cy5** within the cells were observed, with noticeably stronger signals after longer treatment times. This indicates that both types of Dex-conjugates can be endocytosed by LNCaP cells. The process runs slightly faster for **Dex-TCT-GuL-Cy5**, which was observed after 30 min of incubation. When considering the percentage of GuL substitution, it is hard to draw conclusions over its role in cell binding as long as the difference in signal strength between 50% GuL and 5% GuL substituted PAD or Dex-TCT is not well pronounced. Further investigation revealed that the presence of GuL in **PAD** based formulations was not enough to provide binding specificity. After incubation with PSMA negative PC3 cells, **PAD-GUL-Cy5** was still subject to endocytosis; this is in contrast to **Dex-TCT-GuL-Cy5**, which gave no signal. This observation was confirmed in additional experiments on LNCaP cells preincubated with PSMA inhibitor 2-PMPA (1 mM), which prevented attachment of **Dex-TCT-GuL-Cy5** to the receptor but remained with no significant influence on **PAD-GuL-Cy5** endocytosis. Finally, LNCaP cell treatment at 4 °C blocked unspecific binding of **PAD-GuL-Cy5**, whereas selective recognition of **Dex-TCT-GuL-Cy5** by PSMA could take place, though could not be followed by internalization.

4.5. Radiolabelling and serum stability

The complexes of ^{177}Lu-labelled Dex-conjugates were prepared with specific activity from 40 to 200 MBq/mg. The radiolabeling yield obtained for DX-TCT formulations was higher than 99% and was better than for PAD formulation which hovers around 90%. The radiochemical stability for all Dex-conjugation was determined in radiolabeling buffer (AAB). More beneficial radiochemical stability in human blood serum was observed for DX-TCT formulations (up to 6 days) compared to PAD formulations, which decrease after 48 h below 95%, (Table 2).

5. Discussion

We have successfully obtained two types of formulation based on the dextran chain. **PAD**-based formulations folded into micelle-like structured nanoparticles, while Dex-TCT conjugates showed no organized structure. NPs showed hydrodynamic diameter mode values between 80 and 150 nm depending on the amount of added PSMA-inhibitor and DOTA. There was a noticeable trend of decreasing mode value with increasing amount of PEG-GuL-NH2 and decreasing DOTA content. This might be caused by stronger coiling due to present of PEG chains, as well as reduced steric hindrance of DOTA molecules interfering in the NPs structure. Zeta potential was also found to decrease with increasing content of GuL, probably due to the greater substitution of amine groups on the coiling agent (DAD).

Dex-TCT-GuL-DOTA conjugates showed significantly higher levels of DOTA attached when compared to the corresponding **PAD-GuL** NPs. The attachment of DOTA to previously activated dextran chain with TCT results in highly stable linkage, while conjugation of DOTA to the **PAD-GuL** NPs requires additional reduction of the DAD-PAD Schiff base. Consequently, the remaining unreacted Schiff-bases are unstable and responsible for the DOTA detachment. This was observed in the radiolabeling studies, where both types of formulation exhibited good radiolabeling properties. However, for **PAD-GuL-DOTA** NPs, decreasing radiostability over time was observed, while **Dex-TCT-GuL-DOTA** showed excellent radiolabeling purity and stability. Still, once radiolabeled, both types of obtained formulation showed stability over 90% after 48 h in both radiolabeling buffer and human serum. Compared to radiocarriers previously reported in the literature, the obtained formulations are bind the isotope with higher efficacy.

PSMA inhibition data showed that both PAD-DOTA NPs and Dex-TCT-DOTA without GuL showed almost no inhibition. The highest inhibition was recorded for Dex-TCT-50%GuL-DOTA and surprisingly for **PAD-30%GuL-DOTA** instead of **PAD-50%GuL-DOTA**. Also, **PAD-5% GuL-DOTA** showed higher inhibition than **Dex-TCT-GuL-DOTA** with the same theoretical GuL content. It may indicate that additional mechanisms occur in the case of nanoparticles; this is also reflected in the GuL 0% samples, where **PAD** inhibition is slightly elevated in the highest concentration. The endocytic pathway and GuL–PSMA interactions were observed in cell assays for both types of formulation. **Dex-TCT-GuL-DOTA** formulations showed highly specific bonding with PSMA receptor. PSMA + cells showed high binding of **Dex-TCT-GuL-DOTA**, whereas PSMA-cells and PSMA + preincubated with 2-PMPA inhibitor showed nearly no binding of conjugates. As mentioned above, NPs were endocytosed in both cases independently from PSMA receptor availability, using a different endocytic pathway. It appears that the tertiary structure of dextran in the nanoparticles significantly influences NPs interactions with cells and undergoes different endocytic mechanisms when compared to the free dextran chains. Furthermore, based on these observations we can conclude that NPs in used concentrations remain as micelles and are above the CMC value.

Neither **PAD** NPs nor Dex-TCT conjugates showed toxicity on the tested cell lines. This ensures the safety of the obtained radiocarrier, which is vital for future clinical application.

6. Conclusions

In this work, we developed two types of radiocarriers, where **Dex-TCT-GuL** conjugates showed high selectivity towards PSMA receptors in vitro, excellent radiolabeling characteristics and lack of cytotoxicity. It indicates that such formulations might be further used as actively targeted radiopharmaceuticals for either diagnostics or therapy. We believe that the presented conjugates enrich the state-of-the-art and could be further developed for clinical use.

Declaration of competing interest

The authors declare the following financial interests/personal relationships which may be considered as potential competing interests: Janczewska M., Szkop M., Pikus G., Kopyra K., Świątkowska A., Brygoła K., Walczak J., Żuk M.T., Duszak J. and Ciach T. has received salary from NanoThea Inc. This, however, does not alter the authors' adherence to Applied Radiation and Isotopes on sharing the data.

Acknowledgements

This work was supported by the 1.2. Regional Operational Program of the Masovian Voivodeship for the years 2014–2020 [grant numbers: RPMA.01.02.00-14-5723/16] granted to NanoThea Inc. Presented studies have been the base for patent: PCT application PCTIB2019052218 filed by NanoThea Inc. We also thank Aidan McFord and Olly Bayley for language editing of this article.

References

Almasi, T., Jabbari, K., Gholipour, N., Kheirabadi, A.M., Beiki, D., Shahrokhi, P., Akhlaghi, M., 2019. Synthesis, characterization, and in vitro and in vivo ^{68}Ga radiolabeling of thiosemicarbazone Schiff base derived from dialdehyde dextran as a promising blood pool imaging agent. Int. J. Biol. Macromol. https://doi.org/10.1016/j.ijbiomac.2018.12.133.

Corot, C., Schaefer, M., Beaute, S., Bourrinet, P., Zehaf, S., Benize, V., Sabatou, M., Meyer, D., 1997. Physical, chemical and biological evaluations of CMD-A2-Gd-DOTA. A new paramagnetic dextran polymer. Acta Radiol. Suppl. 412, 91–92.

Du, J., Marquez, M., Hiltunen, J., Nilsson, S., Holmberg, A.R., 2000. Radiolabeling of dextran with rhenium-188. Appl. Radiat. Isot. https://doi.org/10.1016/S0969-8043(99)00283-3.

Gholipour, N., Akhlaghi, M., Kheirabadi, A.M., Ramandi, M.F., Farashahi, A., Beiki, D., Jalilian, A.R., 2019. Development of a novel ^{68}Ga-dextran carboxylate derivative for blood pool imaging. Radiochim. Acta. https://doi.org/10.1515/ract-2018-2959.

Gracia, R., Marradi, M., Cossio, U., Benito, A., Perez-San Vincente, A., Gomez-Vallejo, V., Grande, H.-J., Llop, J., Loinaz, I., 2017. Synthesis and functionalization of dextran–based single–chain nanoparticles in aqueous media. J. Mat. Chem. B. https://doi.org/10.1039/C9CC00924H.

Holmberg, A.R., Marquez, M., Lennartsson, L., Meurling, L., Nilsson, S., 2018. Synthesis and binding of a novel PSMA-specific conjugate. Anticancer Res. 38, 1531–1537.

Jarrett, B.R., Gustafsson, B., Kukis, D.L., Louie, A.Y., 2008. Synthesis of ^{64}Cu-labeled magnetic nanoparticles for multimodal imaging. Bioconjugate Chem. 19 (7), 1496–1504.

Liberti, M.V., Locasale, J.W., 2016. The Warburg effect: how does it benefit cancer cells? Trends Biochem. Sci. https://doi.org/10.1016/j.tibs.2015.12.001.

Petter, A.H., Per, C.S., Eckart, H., Jo, K., Pal, R., 2013. In vivo cleavage rate of a dextran-bound magnetic resonance imaging contrast agent: preparation and intravascular pharmacokinetic characteristics in the rabbit. Curr. Drug Deliv. 10 (1), 134–143.

Szkop, M., Brygoła, K., Janczewska, M., Ciach, T., 2019. A simple time-resolved fluorescence assay for quantitative determination of DOTA chelator. Anal. Biochem. https://doi.org/10.1016/j.ab.2019.113384.

Zhang, J., Smith, K.M., Tackaberry, T., Sun, X., Carpenter, P., Slugowski, M.D., Robins, M.J., Nielsen, L.P., Nowak, I., Baldwin, S.A., Young, J.D., Cass, C.E., 2006. Characterization of the transport mechanism and permeant binding profile of the uridine permease Fui1p of Saccharomyces cerevisiae. J. Biol. Chem. 281 (38), 28210–28221.